ARTICLE

doi:10.1038/nature11691

Automated design of ligands to polypharmacological profiles

Jérémy Besnard[1], Gian Filippo Ruda [1], Vincent Setola[2], Keren Abecassis[1], Ramona M. Rodriguiz[3], Xi-Ping Huang[2], Suzanne Norval[1], Maria F. Sassano[4], Antony I. Shin[3], Lauren A. Webster[1], Frederick R. C. Simeons[1], Laste Stojanovski[1], Annik Prat[5], Nabil G. Seidah[5], Daniel B. Constam[6], G. Richard Bickerton[1], Kevin D. Read[1], William C. Wetsel[3,7], Ian H. Gilbert[1], Bryan L. Roth[2,4] & Andrew L. Hopkins[1]

The clinical efficacy and safety of a drug is determined by its activity profile across many proteins in the proteome. However, designing drugs with a specific multi-target profile is both complex and difficult. Therefore methods to design drugs rationally a priori against profiles of several proteins would have immense value in drug discovery. Here we describe a new approach for the automated design of ligands against profiles of multiple drug targets. The method is demonstrated by the evolution of an approved acetylcholinesterase inhibitor drug into brain-penetrable ligands with either specific polypharmacology or exquisite selectivity profiles for G-protein-coupled receptors. Overall, 800 ligand–target predictions of prospectively designed ligands were tested experimentally, of which 75% were confirmed to be correct. We also demonstrate target engagement *in vivo*. The approach can be a useful source of drug leads when multi-target profiles are required to achieve either selectivity over other drug targets or a desired polypharmacology.

The safety and efficacy of a drug is determined not only by its action on an individual protein, but also by its interactions with many proteins in the proteome. The promiscuous interaction of a drug with undesired proteins frequently causes toxicity[1] and adverse effects[2,3]. Conversely, a single drug target can be therapeutically insufficient, particularly in complex neuropsychiatric conditions, infectious diseases or cancer[4–6]. Instead, it is frequently necessary for a drug to engage two or more targets simultaneously for therapeutic efficacy[7]. Psychiatric drugs in particular require multiple activities against several targets to modulate therapeutically complex neuropsychiatric domains including perception, cognition and emotion[4]. However, designing drugs with a specific multi-target profile—to achieve either exquisite selectivity over other drug targets or a desired polypharmacology—is a complex and exceedingly difficult task for medicinal chemistry[8]. Accordingly, methods are needed to enable drugs to be designed a priori against several molecular targets simultaneously. Here we describe a solution to the complex problem of designing ligands against multiple drug target profiles by automated design.

From prediction to design

The problem of designing ligands against a multi-target profile involves the parallel optimization of multiple structure–activity relationships within a desired range of physicochemical properties. The prospect of multi-target drug design has been recently aided by the development of computational methods that show success in predicting the molecular targets of drugs[3,9–13] (Supplementary Fig. 1), although such approaches are not intrinsically design methods.

Drug design can be modelled as an evolutionary process of iterative cycles of exploration and analysis[14,15]. Adaptive design processes are efficient at solving complex, multi-objective problems. Accordingly, we developed an automated, adaptive design approach to optimize ligands against polypharmacological profiles.

Several *de novo* drug design methods have been proposed previously[16–21]. However, of those that have been experimentally tested[22–26], high affinity ligands have been described only rarely and these are all against a single molecular target objective[24,26]. In contrast to previous *de novo* approaches, we mimicked the creative process by automated learning of medicinal chemistry design tactics, applying these automated learning approaches to the generation of analogues, and then prioritizing them relative to a set of objectives (Fig. 1a). The development of this approach is described below, starting from 'off-target' predictions, progressing to ligand design, and finally to the discovery of novel compounds with predefined multi-target profiles.

Evolution of a drug

James Black proposed that, "the most fruitful basis for the discovery of a new drug is to start with an old drug"[27]. Accordingly, we tested whether the algorithm could automate the evolution of new biological activities, starting from a known drug. Donepezil (compound **1**) is an acetylcholinesterase inhibitor approved for cognitive enhancement in Alzheimer's disease. Bayesian probabilistic activity models[9], for 784 molecular targets built from the ChEMBL database[28], predicted a moderate likelihood that donepezil possessed D4 dopamine receptor activity and a low chance of D2 dopamine receptor activity (Supplementary Table 1). We found donepezil was a moderately potent D4 inverse agonist (inhibition constant $K_i = 614$ nM) with minimal D2 activity (Supplementary Figs 2 and 3 and Supplementary Tables 2 and 3). The D4 inverse agonist activity of donepezil is intriguing given analyses demonstrating a significant improvement in memory in the trail making test with this drug[29] and findings that D4 antagonists can prevent stress-induced cognitive dysfunction in primates[30].

We tested our method by evolving the structure of donepezil with the dual objectives of improving D2 activity and achieving blood–brain

[1]Division of Biological Chemistry and Drug Discovery, College of Life Sciences, University of Dundee, Dundee DD1 5EH, UK. [2]NIMH Psychoactive Drug Screening Program, Department of Pharmacology, The University of North Carolina Chapel Hill School of Medicine, Chapel Hill, North Carolina 27759, USA. [3]Mouse Behavioral and Neuroendocrine Analysis Core Facility, Duke University Medical School, Durham, North Carolina 27710, USA. [4]Department of Pharmacology and Division of Chemical Biology and Medicinal Chemistry, The University of North Carolina Chapel Hill School of Medicine, Chapel Hill, North Carolina 27759, USA. [5]Laboratory of Biochemical Neuroendocrinology, Clinical Research Institute of Montreal (IRCM), affiliated with the University of Montreal, Montreal, Quebec, H2W 1R7, Canada. [6]Ecole Polytechnique Fédérale de Lausanne (EPFL) SV ISREC, Station 19, CH-1015 Lausanne, Switzerland. [7]Departments of Psychiatry and Behavioral Sciences, Cell Biology, and Neurobiology, Duke University Medical School, Durham, North Carolina 27710, USA.

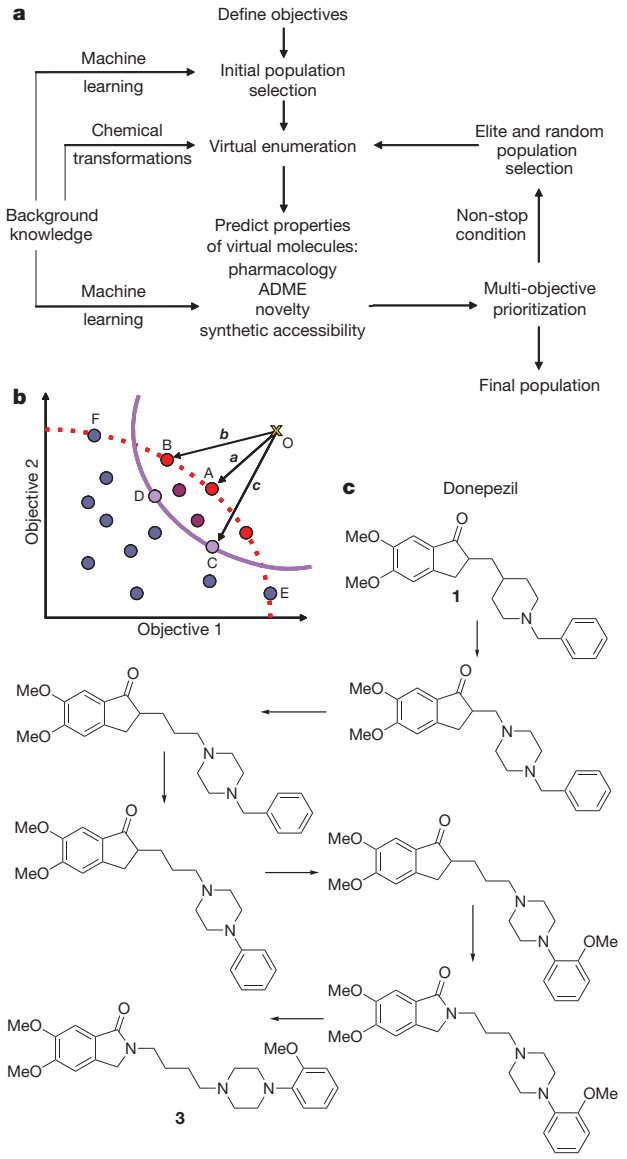

Figure 1 | Adaptive drug design. **a**, Closed loop of automated ligand design algorithm by multi-objective evolutionary optimization. **b**, Multi-objective prioritization by vector scalarization. The multi-target objectives are defined as the coordinates of the ideal achievement point, O (gold cross), and the predicted values of each generated compound (coloured circles) are also defined as coordinates in a multi-dimensional space. The Pareto frontier is displayed as a red dotted line. The multi-objective prioritization is inverse to the magnitude of vectors ($||a|| < ||b|| < ||c||$). Compound A is prioritized the highest. Compounds C and D have the same vector length ($||c|| = ||d||$) and are thus prioritized equally and above the Pareto optimal compounds E and F. **c,** Evolution of donepezil (compound **1**) (19% inhibition of D2 receptor at 10 μM; D2 dopamine Bayesian score = 25) into D2 dopamine inverse agonist compound **3** (96% inhibition of D2 receptor at 10 μM; D2 dopamine Bayesian score = 92). The Tanimoto similarity between donepezil and compound **3** is only 0.35.

barrier penetration. In our approach the desired multi-objective profile is defined a priori and then expressed as a point in multi-dimensional space termed 'the ideal achievement point'. In this first example the objectives were simply defined as two target properties and therefore the space has two dimensions. Each dimension is defined by a Bayesian score for the predicted activity and a combined score that describes the absorption, distribution, metabolism and excretion (ADME) properties suitable for blood–brain barrier penetration (D2 score = 100, ADME score = 50). We then generated alternative chemical structures by a set of structural transformations using donepezil as the starting structure. The population was subsequently enumerated by applying a set of transformations to the parent compound(s) of each generation. In contrast to rules-based or synthetic-reaction-based approaches for generating chemical structures[16,31–34], we used a knowledge-based approach by mining the medicinal chemistry literature[28,35]. By deriving structural transformations from medicinal chemistry, we attempted to mimic the creative design process[36] (Supplementary Fig. 4). Activity predictions were calculated for each of the enumerated compounds from all Bayesian models. Scores representing the likelihood of central nervous system (CNS) penetration and good ADME properties were calculated using the program StarDrop and combined into a single value. The predicted properties of the enumerated structures were then expressed as points in multi-dimensional space. The generated structures were subsequently ranked by the distance (in multi-dimensional space) between the predicted properties for each structure and the ideal achievement point[37] (Fig. 1b). Compounds were filtered for novelty, Lipinski's rule of five compliance[38] and synthetic accessibility[39]. The top 10,000 prioritized structures were selected for the next iterative cycle along with 500 random structures from the remaining population. The process was iterated until either a structure close to the objectives was discovered or no further improvements were achieved.

Initially, we evolved a series of isoindoles and prioritized them using our achievement objectives as criteria (Fig. 1c, Supplementary Table 4 and Supplementary Fig. 5). Eight analogues were then synthesized and tested (Fig. 2, Supplementary Figs 2 and 6 and Supplementary Table 5), with all showing substantial D2 receptor affinities (K_i values = 156–1,700 nM, Supplementary Table 3).

The second highest ranking compound (compound **3**)—chosen from the final population of evolved structures —exhibited the highest D2 receptor affinity (K_i = 156 nM). Thus, we successfully evolved the negligible D2 receptor binding activity of donepezil into a series of ligands with higher D2 affinities (Fig. 2). Functionally, compound **3** was a dual D2 inverse agonist and D4 agonist (Supplementary Fig. 3). CNS penetration studies showed that compound **3** penetrates the brain as predicted, with an *in vivo* brain–blood ratio (BBR) of 0.5.

Although the evolved compounds were selected for the D2 receptor objective, other predicted activities were not selected against. Accordingly, each of the generated compounds had a predicted polypharmacology profile. In general, this set of isoindole analogues was predicted to exhibit promiscuous profiles, with variable activities predicted for multiple serotonergic, adrenergic and dopaminergic receptor subtypes (Supplementary Tables 1 and 5). These predicted promiscuous profiles were subsequently confirmed (Fig. 2 and Supplementary Tables 2 and 3), and the predicted multi-target profiles displayed excellent agreement with experimentally determined profiles, thereby implying that the approach can be applied to the *de novo* design of multi-target agents.

Reducing anti-target activity

The isoindoles exhibited moderately potent affinities for the α_1-adrenoceptors (K_i values = 0.9–3,577 nM, mean K_i = 277 nM, Supplementary Table 3 and Supplementary Fig. 2). Because α_1-adrenoceptor antagonists can induce low blood pressure as a side effect they are considered 'anti-targets' to be avoided in drug design[40]. A common drug design optimization problem is to reduce such anti-target activity while maintaining desired on-target activities. We accordingly evolved the eight newly synthesized isoindoles towards a polypharmacological profile (5-HT_{1A} serotonin receptor and D2-, D3- and D4-dopamine receptors) with selectivity over the three α_1-adrenoreceptors anti-targets (α_{1A}, α_{1B} and α_{1D}) while maintaining CNS penetration.

To compare evolutionary strategies, the isoindoles were optimized towards polypharmacology objectives with and without highly predicted α_1 activities filtered-out at each generation (Fig. 3a and Supplementary Fig. 7 and Supplementary Tables 6 and 7). In both optimizations benzolactams were ranked the highest (compounds **11a** and **10a** respectively) (Fig. 3b and Supplementary Tables 6 and

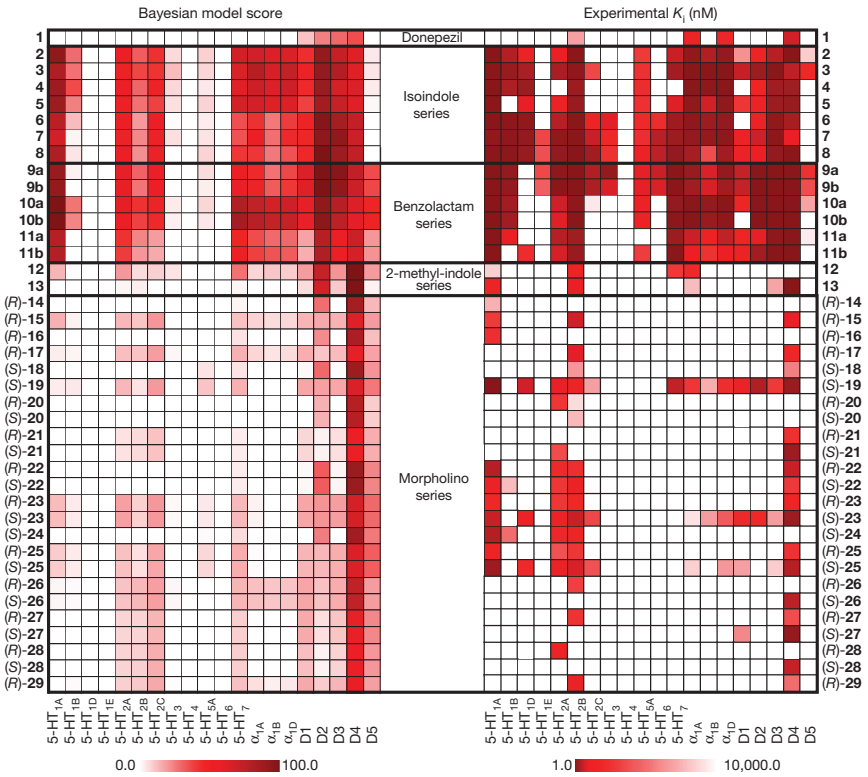

Figure 2 | Polypharmacology profiles of designed ligands. Comparison of the predicted Bayesian and observed polypharmacology profiles for (1) donepezil (compound **1**); (2) the isoindole analogues (compounds **2**–**8**)—of the 160 ligand–target associations, 100 were correctly predicted by the Bayesian models ($P = 0.001$; probability of success of 0.63 with 95% confidence intervals of 0.55–0.70); (3) the benzolactam analogues (compounds **9a**–**11b**)—of the 160 ligand–target associations, 107 were correctly predicted ($P = 1.1 \times 10^{-5}$); (4) the 2,3-dihydro-indol-1-yl analogues (compounds **12** and **13**); and (5) the morpholino analogues (compounds 14–29)—of the 540 ligand–target associations, 437 were correctly predicted ($P < 2.2 \times 10^{-16}$). The figure is composed of data in Supplementary Tables 1 and 3. In total, of the 800 predictions in the matrix on 39 novel, prospectively designed ligands and donepezil, 599 were experimentally confirmed correct ($P < 2.2 \times 10^{-16}$), with a probability of success of 0.75 (95% confidence interval of 0.72–0.78).

7). Six benzolactam analogues were then synthesized on the basis of both sets of objectives (Supplementary Table 8 and Supplementary Fig. 5). Analogues of the benzo-δ-lactam (3,4,-dihydroisoquinolin-1(2H)-one) (compounds **9a**, **10a** and **11a**) and benzo-ε-lactam (2,3,4,5-tetrahydro-1-H-benzo[c]azepin-1-one) (compounds **9b**, **10b** and **11b**) were synthesized for comparison because both ring systems were highly prioritized.

Both the predicted and observed receptor activity profiles for the synthesized benzolactams are shown in Fig. 3b (see also Supplementary Tables 1 and 3 and Supplementary Fig. 2). The 2-pyridine-piperazine analogues (compounds **11a** and **11b**) have the lowest α_1 predictions and, indeed, exhibited the lowest α_1 affinities (mean $K_i = 1{,}131$ nM). In agreement with the models, compounds **11a** and **11b** also have the lowest affinity for all D2-like dopamine receptors of the benzolactams tested. The dichloro-phenylpiperazine analogues (compounds **9a** and **9b**) exhibited slightly higher α_1 and D2 binding predictions, which were also confirmed experimentally. By contrast, the 2-methoxy phenylpiperazine analogues (compounds **10a** and **10b**) exhibited potent affinities against the polypharmacology profile of 5-HT_{1A}, D2, D3 and D4 receptors, but also had the highest α_1 predictions and were confirmed as the most potent against the α_1 receptors (mean $K_i = 45.3$ nM) (Fig. 3b). Receptor profiling of the benzolactam series revealed that compared to the isoindoles, from which the compounds were evolved, the benzolactams achieved the objective of an increased polypharmacology profile for 5-HT_{1A}, D2, D3 and D4 receptors compared with the α_1-adrenoceptors (Fig. 3b). The benzolactams are 11-fold more selective with respect to D2 receptors and 25-fold more selective with respect to the polypharmacology profile than the isoindoles. Notably, the benzolactam compound **9a** penetrated the brain, (BBR = 5.9), as predicted.

As the benzolactam series was not present in the ChEMBL database (release 1) used to build the Bayesian models, they constituted a novel chemical series for the system to discover[41]. Notably, benzolactam derivatives have recently been independently synthesized and tested as potent D2 and D3 ligands[42]; however, the broader receptor profiles of the compounds were not evaluated. This observation provides additional verification that the algorithm is capable of generating and prioritizing novel chemical structures equivalent to those devised by medicinal chemists.

Potency optimization

We next explored selectivity in the context of our multi-target objectives and asked whether we could optimize potent, selective, CNS-penetrant D4 receptor ligands starting from the chemical structure of donepezil. We executed the optimization in two stages; first we optimized for D4 potency and brain penetrability (Fig. 4a), and then for D4 selectivity (Fig. 4b). A series of 2-methylindoline derivatives with predicted high D4 activity was evolved from donepezil after six generations (Fig. 4a and Supplementary Fig. 9). Notably, compounds belonging to a 2,3-dihydro-indol-1-yl chemotype were dominant in the prioritized set (Supplementary Table 9). Compounds **12** and **13**, which both belong to the 2,3-dihydro-indol-1-yl class, were then selected for testing (Supplementary Figs 5 and 8). The highest ranking compound, **12**, was inactive, whereas compound **13**, the third-highest-ranking design out of the final population, was the most potent D4 ligand among all tested compounds (D4 $K_i = 8.9$ nM). Through the process of optimization, compound **13** represents a 69-fold increase in affinity over donepezil. In contrast to the isoindole and benzolactams analogues, compound **13** is predicted to be a highly selective D4 ligand with 95-fold selectivity over 5-HT_{2B} and weak affinities greater than 1 μM for only five other receptors in our panel of G-protein-coupled receptors (GPCRs) (Fig. 2). Importantly, and as predicted, compound **13** is highly CNS penetrant (BBR = 7.5).

To verify that the predicted properties of selectivity, potency and CNS penetration resulted in D4 receptor activity *in vivo*, we evaluated the effects of compound **13** treatment on behaviour in wild-type and D4 receptor knockout (D4R-KO) mice (Fig. 4c–f), as well as in pro-protein convertase 7 (PC7 encoded by *Pcsk7)* knockout mice (Supplementary Fig. 10a–d) that display a similar D4R-KO phenotype. Although open field locomotor activity declined in vehicle-treated D4R wild-type (DR4-WT) animals (Fig. 4c), it remained high and showed little habituation in D4R-KO mice. Although the treatment with 0.7 mg kg^{-1} of compound **13** was without significant effect in either genotype, the 1 mg kg^{-1} dose reduced locomotion at 0–20 min

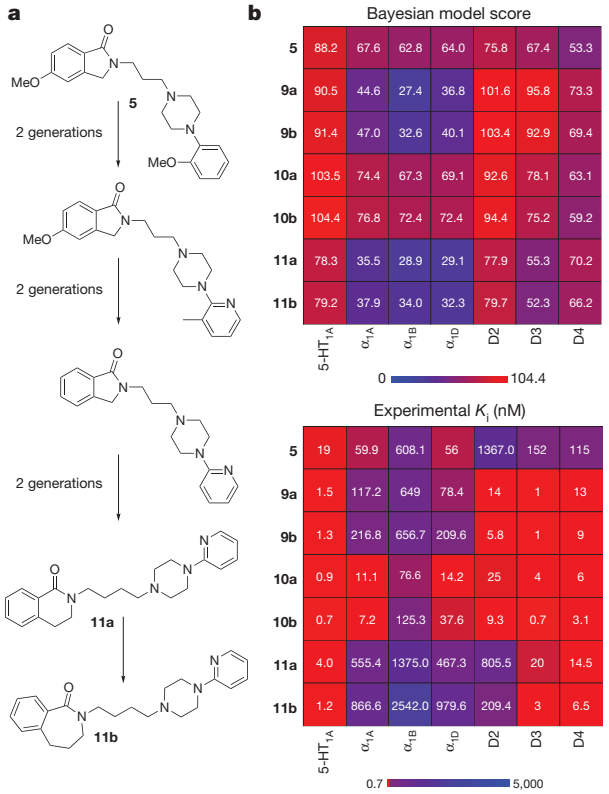

Figure 3 | Reducing α_1 anti-target activity by evolutionary design. **a**, Summary of the evolution of the prioritized benzolactam analogues (compounds **11a** and **11b**) from a parent isoindole analogue (compound **5**). The full evolutionary pathway from compound **5** to **11b** is shown in Supplementary Fig. 7. **b**, Comparison of polypharmacology profiles for the Bayesian model score and experimental binding affinities (K_i) of compound **5** and benzolactam analogues (compounds **9a**–**11b**) for the seven target objectives (α_{1A}, α_{1B} and α_{1D} compared to 5-HT_{1A}, D2, D3 and D4 receptors). On average, the selectivity ratios for the D2, D3, D4 and 5-HT_{1A} receptors for the synthesized benzolactams over the α_1 receptors are 2.8-, 59-, 58- and 312-fold, respectively. In comparison, the average selectivity ratios for D2, D3, D4 and 5-HT_{1A} receptors for the isoindole analogues over the α_1 receptors are 0.27-, 2.1-, 1- and 14-fold, respectively. With respect to the algorithm prioritization for the benzolactam analogues (Supplementary Table 8) against the multi-target objectives, the order of prioritization matches the experimentally determined order for the analogues (dichloro phenylpiperazine > 2-methoxy phenylpiperazine > 2-pyridine piperazine).

in D4R-WT animals. The same dose had no effect in D4R-KO mice. In the centre zone, vehicle-treated D4R-KO mice spent more time in this area at 21–60 min than D4R-WT controls (Fig. 4d). Centre time in D4R-WT animals was enhanced at 0–20 min with both doses of compound **13**; in D4R-KO mice it was attenuated at 41–60 min with the 1 mg kg^{-1} dose. In the hole-board test, head-poking was increased in vehicle-treated D4R-KO animals compared to D4R-WT controls (Fig. 4e). In D4R-WT mice compound **13** augmented head-pokes in a dose-dependent fashion; only the 1 mg kg^{-1} dose attenuated head-poking in mutants. In the zero maze, open-area time was increased in vehicle-treated D4R-KO mice relative to D4R-WT controls (Fig. 4f). Treatment of 1 mg kg^{-1} of compound **13** selectively increased D4R-WT open-area times to similar levels seen with the D4R-KO mice. With regards to PC7 mice, PC7-WT and D4R-WT responses were similar (Supplementary Fig. 8a–d). Although behaviours in PC7-KO vehicle controls essentially phenocopied those in vehicle-treated D4R-KO mice, compound **13** normalized PC7-KO responses to those of PC7-WT controls. By comparison, D4R-KO mice were largely unresponsive to compound **13**—demonstrating high D4R selectivity. Nonetheless, compound **13** did not seem to be absolutely selective because in D4R-KO animals the 1 mg kg^{-1} dose attenuated head-poking in the hole-board test, implying some possible off-target actions at increased doses.

Automated invention

Using compound **13**, we further expanded our objective to evolve ligands that were highly selective for D4 dopamine, CNS penetrant and a new chemotype. The evolution of compound **13** against these objectives resulted in the design of new morpholino compounds (Fig. 4b and Supplementary Fig. 11 and Supplementary Tables 10 and 11). Compounds with the new isoindol-1-yl-ethyl-morpholino backbone were prominent in the prioritized final generation population of 10,000 structures (ranked fifth, sixth and ninth of the top 10 compounds in Supplementary Table 10), whereas most known D4 ligands are 1,4-disubstituted aromatic piperidines and piperazines (1,4-DAPs). However 1,4-DAPs are rather promiscuous substructures common in ligands for many biogenic amine GPCRs[43]. Therefore, the isoindol-1-yl-ethyl-morpholino analogues represent a new D4 chemotype.

A library of 24 morpholino analogues (compounds 14–29) was then synthesized and profiled against our GPCR panel (Supplementary Table 11 and Supplementary Fig. 5). Individual *R* and *S* morpholino enantiomers were synthesized and assayed separately (chirality designated by prefix). To reduce complexity further, direct analogues with and without the carbonyl oxygen were synthesized (for example, compounds **20** and **21**), as this atom was not predicted to be essential to the overall D4 selectivity profile (Fig. 2).

The assays confirmed the predictions that the new morpholino compounds are generally highly selective for the D4 receptor compared with the other tested receptors (Fig. 2). Seventeen of the compounds had affinities for the D4 dopamine receptor, ranging from $K_i = 90$ nM (compound (*S*)-**27**) to $K_i = 5{,}526$ nM (compound (*S*)-**18**) with eight exhibiting affinities less than 1 μM for D4 (compounds (*R*)-**15**, (*S*)-**19**, (*S*)-**21**, (*R*)-**22**, (*S*)-**23**, (*S*)-**26**, (*S*)-**27** and (*S*)-**28**). Compounds containing the ethanone linker-group were generally less active than those with the ethyl linker. For compounds with the ethyl linker, the *S* enantiomer was more potent than the *R* enantiomer. Functional assays of an exemplar compound (*R*)-**22** indicated inverse agonism at the D4 receptor (Supplementary Fig. 3).

In agreement with the design objectives, the morpholinos displayed exquisite selectivity for the D4 dopamine receptor. Excluding the dopamine receptors, low positive Bayesian scores were observed for eight of the compounds against 5-HT_{1A} serotonin receptors, 16 of the compounds against the 5-$HT_{2A/B/C}$ serotonin receptors, and almost all had very low scores for 5-HT_7 serotonin receptors. The off-target trends were confirmed when the compounds were profiled (Fig. 2). The morpholino compounds, on average, bound to 3.4 targets (including D4 at $K_i < 10$ μM) compared to 15.8 targets for the isoindole and benzolactam compounds. Seven of the active compounds had off-target activities for only 1 of the 20 receptors tested. Compound (*S*)-**26** is the most selective compound with no measured affinity for any other screened receptor. Four compounds possessed both relatively high affinity (D4 $K_i < 1$ μM) and two or fewer off-target activities out of the 20 GPCRs profiled ((*S*)-**21**, (*S*)-**26**, (*S*)-**27** and (*S*)-**28**).

The morpholino series thus represents a new class of highly selective, brain-penetrant, D4 dopamine receptor ligands. Compounds (*S*)-**27** (D4 $K_i = 90$ nM; D1 $K_i = 5852$ nM; BBR = 2.0) and (*S*)-**21** (D4 $K_i = 182$ nM, 5-HT_{2A} $K_i = 3{,}545$ nM) qualified as lead compounds that fulfilled all of our design objectives of novelty, high affinity for the D4 dopamine receptor, exquisite selectivity and CNS penetration. Clearly the automated design of a new class of ligands with a desired multi-target profile demonstrates that the method is able to generate novel, drug-like lead compounds directly by automated design.

Drug design from knowledge

We focused on the polypharmacology of bioaminergic GPCRs as a convenient test case, owing to the importance of multi-target profiles at these receptors for a variety of neuropsychiatric indications[4]. In

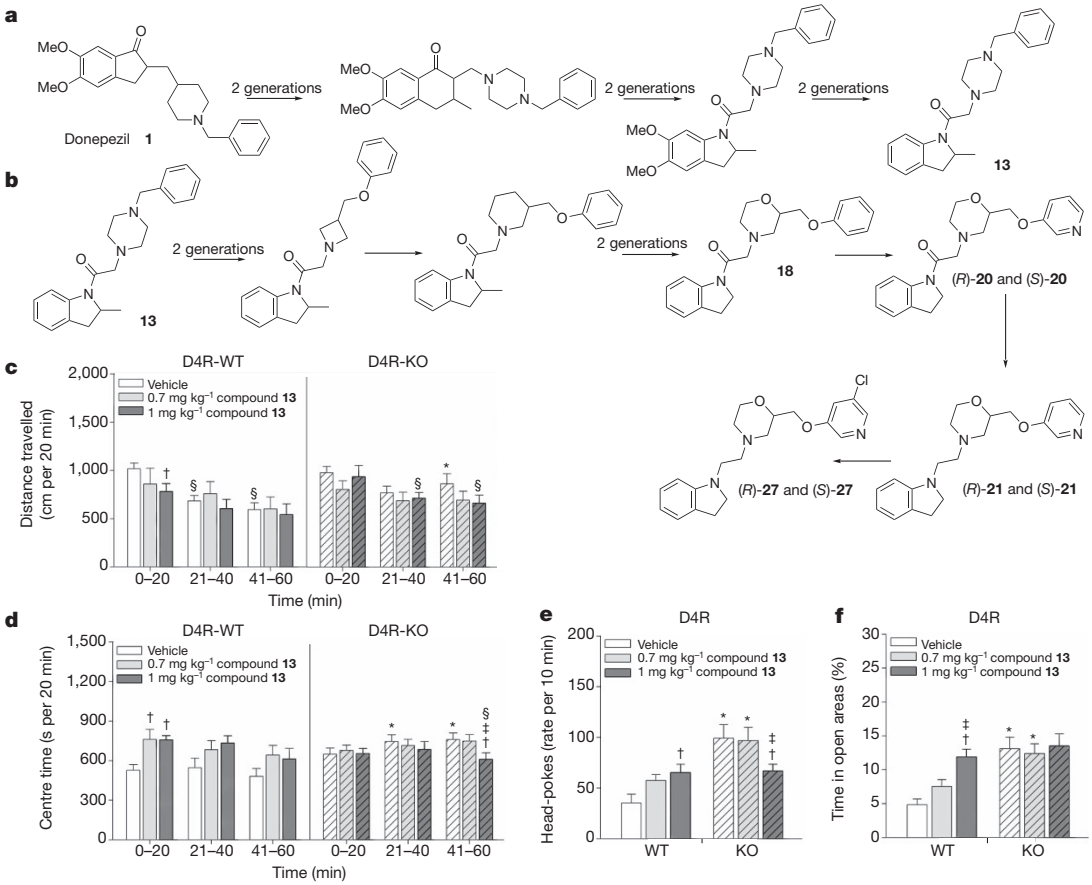

Figure 4 | Evolution of D4 dopamine ligands from donepezil. **a**, Summary of the evolution of donepezil (compound **1**) (D4 dopamine Bayesian score = 26, D4 K_i = 614 nM) into D4 dopamine inverse agonist compound **13** (D4 dopamine Bayesian score = 112, D4 k_i = 8.9 nM). The Tanimoto similarity between donepezil and compound **13** is only 0.26. The full evolutionary pathway from donepezil to compound **13** is shown in Supplementary Fig. 9. **b**, Summary of the evolution of selective novel D4 dopamine ligands. Compound **13** is further evolved by selection for novelty and D4 selectivity into the morpholino analogues **18**, **20** (*R* and *S*), **21** (*R* and *S*) and **27** (*R* and *S*). The full evolutionary pathway from compound **13** to **27** is shown in Supplementary Fig. 11 **c**–**f,** Behavioural analysis of a novel D4 dopamine ligand in D4 receptor knockout (D4R KO) mice. D4R-WT, D4R-wild type. **c,** Distance travelled in the open field over 60 min. Mice were given intraperitoneal injection of vehicle or 0.7 or 1 mg kg^{-1} of compound **13** and tested immediately over 60 min. **d**, Time spent in the centre zone in the open field. **e**, The numbers of head-pokes in the hole-board test. Animals were injected with vehicle or 0.7 or 1 mg kg^{-1} of compound **13** and tested 30 min later over 10 min. **f**, Percentage of time in the open areas in the zero maze in D4R mice. Animals were administered vehicle or compound **13** and tested 30 min later for 5 min. n = 8–14 mice per treatment/condition. *$P < 0.05$, wild-type compared with D4R-KO mice or compared to the D4R-KO mice at the same time-point; †$P < 0.05$, comparisons within genotype to the vehicle; ‡$P < 0.05$, comparisons between 0.7 and 1 mg kg^{-1} compound **13**; §$P < 0.05$, compared to the 0–20 min time-point. All error bars are mean ± s.e.m.

principle, the approach is applicable to all drug–target classes, limited only by the requirement for sufficient structure–activity data to create useful models[9–12]. To extend polypharmacology profiling and hence *de novo* design it will be necessary to develop inference methods to build predictive bioactivity models that integrate all available structure–activity relationships, protein structure and protein sequence information together and combine data from diverse scoring functions into predictive frameworks[44,45].

De novo, automated compound design against multi-target profiles provides a powerful new approach for discovering new ligands and drug leads. The method is particularly useful as a new source of leads for polypharmacology profiles.

METHODS SUMMARY

Adaptive optimization. A library of historical chemical structure transformations was derived by mining the ChEMBL database[28]. Each transformation was systematically applied to every parent compound in each generation. Bayesian activity models[9,46] were calculated for more than 784 proteins based on the ECFP6 fingerprint representation[46] of chemical structures of structure–activity data in ChEMBL. Each compound in every generation was scored against the panel of Bayesian models. ADME properties were calculated using StarDrop (Optibrium). Synthetic accessibility was assessed using a previously published method[39] based on the statistical representation of fragments in ChEMBL and molecular complexity. The algorithm was programmed in Pipeline Pilot (version 7.5, Accelrys).

Chemical synthesis. Details of the purchase, synthesis and purification of all compounds are provided in the Supplementary Information.

Experimental testing. The predicted receptor profiles of all the compounds were assessed using standard radioligand binding and functional assay methods at the National Institute of Mental Health Psychoactive Drug Screening Program. The hERG assay was performed as previously described[47]. Metabolic stability was assessed as previously described[48] and brain penetration was assessed by determining the ratio of tested compound between brain and blood at a set time point following intraperitoneal or intravenous administration. For behavioural studies, compound **13** was dissolved in a 0.1% N,N-dimethylacetamide (DMA) with 15% 2-hydroxypropyl-β-cyclodextrin (Sigma-Aldrich) solution and injected intraperitoneally immediately before placement into the open field or 30 min before the zero-maze or hole-board tests as described[49,50] using AccuScan (AccuScan Instruments), Noldus Observer XT 9.0 (Noldus Technologies), and Clever Sys TopScan software (Clever Sys), respectively. All behavioural data are presented as means ± s.e.m and were analysed with SPSS 20 (IBM). Details of the *in vivo* experiments are described in the Supplementary Information.

Full Methods and any associated references are available in the online version of the paper.

Received 1 April 2011; accepted 19 October 2012.

1. Hughes, J. D. *et al.* Physicochemical drug properties associated with *in vivo* toxicological outcomes. *Bioorg. Med. Chem. Lett.* **18,** 4872–4875 (2008).
2. Roth, B. L. Drugs and valvular heart disease. *N. Engl. J. Med.* **356,** 6–9 (2007).
3. Campillos, M., Kuhn, M., Gavin, A. C., Jensen, L. J. & Bork, P. Drug target identification using side-effect similarity. *Science* **321,** 263–266 (2008).
4. Roth, B. L., Sheffler, D. J. & Kroeze, W. K. Magic shotguns versus magic bullets: selectively non-selective drugs for mood disorders and schizophrenia. *Nature Rev. Drug Discov.* **3,** 353–359 (2004).
5. Knight, Z. A., Lin, H. & Shokat, K. M. Targeting the cancer kinome through polypharmacology. *Nature Rev. Cancer* **10,** 130–137 (2010).
6. Brötz-Oesterhelt, H. & Brunner, N. A. How many modes of action should an antibiotic have? *Curr. Opin. Pharmacol.* **8,** 564–573 (2008).
7. Hopkins, A. L. Network pharmacology: the next paradigm in drug discovery. *Nature Chem. Biol.* **4,** 682–690 (2008).
8. Morphy, R. & Rankovic, Z. Designed multiple ligands. An emerging drug discovery paradigm. *J. Med. Chem.* **48,** 6523–6543 (2005).
9. Paolini, G. V., Shapland, R. H. B., van Hoorn, W. P., Mason, J. S. & Hopkins, A. L. Global mapping of pharmacological space. *Nature Biotechnol.* **24,** 805–815 (2006).
10. Keiser, M. J. *et al.* Relating protein pharmacology by ligand chemistry. *Nature Biotechnol.* **25,** 197–206 (2007).
11. Keiser, M. J. *et al.* Predicting new molecular targets for known drugs. *Nature* **462,** 175–181 (2009).
12. Vidal, D. & Mestres, J. In silico receptorome screening of antipsychotic drugs. *Mol. Inf.* **29,** 543–551 (2010).
13. Lounkine, E. *et al.* Large-scale prediction and testing of drug activity on side-effect targets. *Nature* **486,** 361–367 (2012).
14. Schneider, G. & So, S.-S. *Adaptive Systems in Drug Design* (Landes Biosciences, 2002).
15. Schneider, G. *et al.* Voyages to the (un)known: adaptive design of bioactive compounds. *Trends Biotechnol.* **27,** 18–26 (2009).
16. Schneider, G., Lee, M. L., Stahl, M. & Schneider, P. *De novo* design of molecular architectures by evolutionary assembly of drug-derived building blocks. *J. Comput. Aided Mol. Des.* **14,** 487–494 (2000).
17. Gillet, V. J., Willett, P., Fleming, P. J. & Green, D. V. Designing focused libraries using MoSELECT. *J. Mol. Graph. Model.* **20,** 491–498 (2002).
18. Brown, N., McKay, B. & Gasteiger, J. The *de novo* design of median molecules within a property range of interest. *J. Comput. Aided Mol. Des.* **18,** 761–771 (2004).
19. Nicolaou, C. A., Brown, N. & Pattichis, C. S. Molecular optimization using computational multi-objective methods. *Curr. Opin. Drug Discov. Devel.* **10,** 316–324 (2007).
20. Liu, Q., Masek, B., Smith, K. & Smith, J. Tagged fragment method for evolutionary structure-based de novo lead generation and optimization. *J. Med. Chem.* **50,** 5392–5402 (2007).
21. Dey, F. & Caflisch, A. Fragment-based *de novo* ligand design by multiobjective evolutionary optimization. *J. Chem. Inf. Model.* **48,** 679–690 (2008).
22. Vinkers, H. M. *et al.* SYNOPSIS: SYNthesize and OPtimize system in silico. *J. Med. Chem.* **46,** 2765–2773 (2003).
23. Heikkilä, T. *et al.* The first *de novo* designed inhibitors of *Plasmodium falciparum* dihydroorotate dehydrogenase. *Bioorg. Med. Chem. Lett.* **16,** 88–92 (2006).
24. Roche, O. & Rodríguez Sarmiento, R. M. A new class of histamine H3 receptor antagonists derived from ligand based design. *Bioorg. Med. Chem. Lett.* **17,** 3670–3675 (2007).
25. Alig, L. *et al.* Benzodioxoles: novel cannabinoid-1 receptor inverse agonists for the treatment of obesity. *J. Med. Chem.* **51,** 2115–2127 (2008).
26. Schneider, G. *et al.* Reaction-driven de novo design, synthesis and testing of potential type II kinase inhibitors. *Future Med. Chem.* **3,** 415–424 (2011).
27. Wermuth, C. G. Selective optimization of side activities: the SOSA approach. *Drug Discov. Today* **11,** 160–164 (2006).
28. Gaulton, A. *et al.* ChEMBL: a large-scale bioactivity database for drug discovery. *Nucleic Acids Res.* **40,** D1100–D1107 (2012).
29. Ribeiz, S. R. *et al.* Cholinesterase inhibitors as adjunctive therapy in patients with schizophrenia and schizoaffective disorder: a review and meta-analysis of the literature. *CNS Drugs* **24,** 303–317 (2010).
30. Arnsten, A. F., Murphy, B. & Merchant, K. The selective dopamine D4 receptor antagonist, PNU-101387G, prevents stress-induced cognitive deficits in monkeys. *Neuropsychopharmacology* **23,** 405–410 (2000).
31. Gillet, V., Johnson, A. P., Mata, P., Sike, S. & Williams, P. SPROUT: a program for structure generation. *J. Comput. Aided Mol. Des.* **7,** 127–153 (1993).
32. Stahl, M. *et al.* A validation study on the practical use of automated de novo design. *J. Comput. Aided Mol. Des.* **16,** 459–478 (2002).
33. Brown, N., McKay, B., Gilardoni, F. & Gasteiger, J. A graph-based genetic algorithm and its application to the multiobjective evolution of median molecules. *J. Chem. Inf. Comput. Sci.* **44,** 1079–1087 (2004).
34. Nicolaou, C. A., Apostolakis, J. & Pattichis, C. S. De novo drug design using multiobjective evolutionary graphs. *J. Chem. Inf. Model.* **49,** 295–307 (2009).
35. Stewart, K. D., Shiroda, M. & James, C. A. Drug Guru: a computer software program for drug design using medicinal chemistry rules. *Bioorg. Med. Chem.* **14,** 7011–7022 (2006).
36. Kryssanov, V. V., Tamaki, H. & Kitamura, S. Understanding design fundamentals: how synthesis and analysis drive creativity, resulting in emergence. *Artif. Intell. Eng.* **15,** 329–342 (2001).
37. Deb, K., Sundar, J., Udaya Bhaskara Rao, N. & Chaudhuri, S. Reference point based multi-objective optimization using evolutionary algorithms. *Int. J. Comp. Intell. Res.* **2,** 273–286 (2006).
38. Lipinski, C. A., Lombardo, F., Dominy, B. W. & Feeney, P. J. Experimental and computational approaches to estimate solubility and permeability in drug discovery and development settings. *Adv. Drug Deliv. Rev.* **23,** 3–25 (1997).
39. Ertl, P. & Schuffenhauer, A. Estimation of synthetic accessibility score of drug-like molecules based on molecular complexity and fragment contributions. *J. Cheminform.* **10,** 8 (2009).
40. Fanelli, F. & De Benedetti, P. G. in *Antitargets: Prediction and Prevention of Drug Side Effects* (eds Vaz, R. J. & Klabunde, T.) Ch. 8, 155–193 (Wiley-VCH, 2008).
41. Bemis, G. W. & Murcko, M. A. The properties of known drugs. 1. molecular frameworks. *J. Med. Chem.* **39,** 2887–2893 (1996).
42. Ortega, R. *et al.* Synthesis, binding affinity and SAR of new benzolactam derivatives as dopamine D_3 receptor ligands. *Bioorg. Med. Chem. Lett.* **19,** 1773–1778 (2009).
43. Löber, S., Hübner, H., Tschammer, N. & Gmeiner, P. Recent advances in the search for D_3 and D_4 selective drugs: probes, models and candidates. *Trends Pharmacol. Sci.* **32,** 148–157 (2011).
44. Martin, R. E., Green, L. G., Guba, W., Kratochwil, N. & Christ, A. Discovery of the first nonpeptidic, small-molecule, highly selective somatostatin receptor subtype 5 antagonists: a chemogenomics approach. *J. Med. Chem.* **50,** 6291–6294 (2007).
45. Bender, A. *et al.* Chemogenomic data analysis: prediction of small-molecule targets and the advent of biological fingerprint. *Comb. Chem. High Throughput Screen.* **10,** 719–731 (2007).
46. Rogers, D., Brown, R. D. & Hahn, M. Using extended-connectivity fingerprints with Laplacian-modified Bayesian analysis in high-throughput screening follow-up. *J. Biomol. Screen.* **10,** 682–686 (2005).
47. Huang, X. P., Mangano, T., Hufeisen, S., Setola, V. & Roth, B. L. Identification of human Ether-à-go-go related gene modulators by three screening platforms in an academic drug-discovery setting. *Assay Drug Dev. Technol.* **8,** 727–742 (2010).
48. Ruda, G. F. *et al.* Aryl phosphoramidates of 5-phosho erythronohydroxamic acid, a new class of potent trypanocidal agents. *J. Med. Chem.* **53,** 6071–6078 (2010).
49. Pogorelov, V. M., Rodriguiz, R. M., Insco, M. L., Caron, M. G. & Wetsel, W. C. Novelty seeking and stereotypic activation of behavior in mice with disruption of the *Dat1* gene. *Neuropsychopharmacology.* **30,** 1818–1831 (2005).
50. Porton, B. *et al.* Mice lacking synapsin III show abnormalities in explicit memory and conditioned fear. *Genes Brain Behav.* **9,** 257–268 (2010).

Supplementary Information is available in the online version of the paper.

Acknowledgements This work is supported by SULSA (HR07019), the BBSRC Doctoral Training Programme, the BBSRC Pathfinder (BB/FOF/PF/15/09) and the BBSRC Follow On Fund schemes (BB/J010510/1) (A.L.H.), the University of Dundee's Pump Priming Fund for Translational Medical Research (I.H.G. and A.L.H.) and by grants from the National Institutes of Health (NIH) supporting drug discovery receptor pharmacology (B.L.R.) and the NIH grant MH082441 (W.C.W.). The chemical synthesis and informatics benefits from the infrastructure investments from the Wellcome Trust Strategic Award (WT 083481). We thank J. Overington for StARlite and ChEMBL. We wish to thank D. Murugesan for compound purification and C. Means and T. Rhodes for helping with the open field, hole-board and zero-maze tests. We also wish to thank C. Elms and J. Zhou for their support in the husbandry and generation of the mice used for behavioural testing. We also wish to thank F. Y. Li for customizing the software configuration for the hole-board tests. Some of the equipment used in the behavioural testing was purchased with a grant from the North Carolina Biotechnology Center. B.L.R. also received support from the Michael Hooker Chair of Pharmacology.

Author Contributions A.L.H. devised the method, developed the algorithm and designed the study. J.B. coded the algorithm and undertook the calculations. G.R.B. developed the databases. A.L.H. and J.B. with I.H.G., G.F.R. and K.A. selected the compounds for synthesis. I.H.G., G.F.R. and K.A. designed the synthetic routes and G.F.R. and K.A. undertook the chemical synthesis. L.A.W. purified and analysed several of the compounds. B.L.R. and V.S. designed the empirical tests for the synthesized compound predictions, analysed and interpreted the results and performed the experiments. X.-P.H. performed the 5-HT_{2B} functional assays and the hERG assays. M.F.S. conducted the dopamine D2 and D4 functional assays. K.D.R. designed the drug metabolism and pharmacokinetics studies and analysed the results. S.N., L.S. and F.R.C.S. carried out the DMPK experiments. For the behavioural experiments, D.B.C. created the mice in which the *Pcsk7* gene was disrupted. A.P. and N.G.S. verified the *Pcsk7* deletion in many tissues including brain, and then backcrossed the mice onto a C57BL/6 background. W.C.W. designed the studies; R.M.R. and A.I.S. conducted the experiments and analysed the results; W.C.W., R.M.R., A.I.S., D.B.C., A.P. and N.G.S. interpreted the findings; A.L.H. and B.L.R. wrote the manuscript; I.H.G. wrote the synthetic methods with help from G.F.R., K.A. and L.A.W.; W.C.W. and R.M.R. wrote the behavioural section of the manuscript and J.B., V.S., W.C.W. and R.M.R. prepared the figures. All the authors discussed the results and commented on the manuscript.

Author Information Reprints and permissions information is available at www.nature.com/reprints. The authors declare competing financial interests: details are available in the online version of the paper. Readers are welcome to comment on the online version of the paper. Correspondence and requests for materials should be addressed to A.L.H. (a.hopkins@dundee.ac.uk) or B.L.R. (bryan_roth@med.unc.edu).

METHODS

Data sets. All machine learning and data mining of the medicinal chemistry structure–activity data were conducted on the ChEMBL database (release 1) and a pre-release (StARLite version 31)[28]. The ChEMBL database contains (release 1) more than 440,000 compounds abstracted in *J. Med. Chem.* and *Bioorg. Med. Chem. Lett.* from 1980 to May 2008. The ChEMBL database is available for download from the EBI.

Chemical transformations. A database of chemical transformations was derived from systematically comparing sets of analogue compounds in ChEMBL[28]. Sets of analogues with defined structure–activity relationships were identified in ChEMBL[28] usually from individual journal articles. The transformations database was seeded with a set of common chemical transformations derived from medicinal chemistry knowledge. The transformations database was then expanded by systematically applying all existing transformations to each of the structures associated with each of the journal articles in ChEMBL. The resulting set of transformed compounds was compared to the published analogues. Analogues that were not present in the transformed set highlighted potential transformations that were missing from the transformation database, and were subsequently added to the database. This iterative mining method attempts to regenerate all the reported structures of every medicinal chemistry publication reported in ChEMBL. The chemical transformations were encoded in RXN format. The procedure was implemented in Pipeline Pilot. The current database contains more than 700 unique structural transformations.

Bayesian models. Predictive polypharmacology profiling was undertaken using Bayesian activity models, based on our previously published approach[9]. The Bayesian method for polypharmacology profiling was chosen as it provided both good performance for noisy data sets and a high speed of calculation[51]. High confidence models were built using ChEMBL (release 1). Activity data were filtered to keep only activity end-point points that had half-maximum inhibitory concentration (IC_{50}), half-maximum effective concentration (EC_{50}) or K_i values and where the ChEMBL confidence score was at least seven (protein assignment was direct or a homologue). A compound was considered active when the mean activity value was below 10 μM. All inactive compounds were assigned to the target 'none'. Following this procedure, 133,061 compounds remained with 215,967 activity end-points, which were used for model building. Multiple category Laplacian-modified naive Bayesian models were built with ECFP6 representations[52] for 784 targets. For each model the data were split in two for the validation step: compounds were clustered and assigned a cluster number. Clusters with an odd number were assigned to the test set, and the clusters with an even number were assigned to the training set. Models were built with the training set, and the test set was scored. The training set was scored using its own model as comparison. Finally, a model was built with all data and scored against itself—the training set and whole set should provide similar validation statistics. Statistics on the performance of the models are described in Supplementary Table 12. The results for the model containing all 785 targets were very similar to the models for the receptor subsets. Two analyses were used to assess the performance of the different models. The first analysis provides an overall score and does not need to specify a cut-off for distinguishing active from inactive compounds. The area under the receiver operating characteristic (ROC) curve provides an indication of the ability of the model to prioritize active compounds over inactive compounds. The ROC curve is the plot of the true positive versus the false positive rate. However, it does not provide information on early enrichment, which was important in studies such as the present one in which only the top-ranking compounds were considered. Therefore the Boltzmann-enhanced discrimination of ROC (BEDROC)[53] was used, which solves the early enrichment issue by adding a weight to compounds recognized early. BEDROC was derived from the robust initial enhancement, and the sum of log of ranks test[54], which provided a statistical test to assess which method performs better than random. The percentage of active compound retrieved in the top 5% is also calculated (recall = 5%). The second analysis required a cut-off to make the distinction between active and inactive, as they varied with the rank of the compounds. For each model, the specificity (true negative rate), sensitivity (true positive rate), false positive rate, false negative rate, precision, F-measure and Matthews correlation coefficient (MCC) were calculated at different cut-off values. The cut-off providing the best MCC score was used, as it was shown to provide better performance[55] (Supplementary Fig. 12). The quality of the models was assessed using an internal leave-one-out validation: one compound was part of the test set and was scored using the remaining data as the training set. Then the area under the ROC curve was calculated (Supplementary Fig. 13). A cut-off score was calculated to minimize the sum of the percentage misclassified for category members and for category non-members and used to classify compounds in the contingency table.

An all data model for dopamine receptors only was built using data from a pre-release of ChEMBL (StARLite version 31), with similar numbers of compounds and end-points. The model was built without considering the confidence level of target assignment to gather as much data as possible. This model was used for initial calculation on the evolution of the isoindole series and the 2,3-dihydro-indol-1-yl series. The quality of the models was assessed using the same procedures as described earlier. The results from the all data models and the high confidence models were very similar (for example, D2 models $R^2 = 0.998$, D4 models $R^2 = 0.984$).

Profile prediction probabilities. The cut-off for a good prediction came from the validation steps for the model. From the test set, the cut-off value providing the best MCC value was used. For the $5\text{-}HT_{1E}$ receptor, a cut-off of zero was selected. For each ligand–target association, the probability of success was 0.5 (active or inactive where activity was defined as $K_i < 10\ \mu M$). To test whether the profile predictions were better than random, an exact binomial test was performed using R (version 2.8.1) (http://www.r-project.org), and the cumulative binomial probability was calculated.

Adaptive optimization. The adaptive optimization procedure involves defining a parent population of compounds (P_P), of at least one molecule, and a set of n ideal achievement objectives $\{x_O^1, \ldots, x_O^n\}$, where n is at least 1. The parent population of compounds for each generation (G) is defined as $P_{P(G=n)}$, in which $n = 0$ for the initial population. All of the members of the parent population (P_P) are subjected to all possible transformations, to maximize the pool of molecules in the transformed population (P_T). Each member of the transformed population is scored using the calculated predictions and molecular properties and ranked relative to the achievement objectives $\{x_O^1, \ldots, x_O^n\}$. Pareto ranking is a common method for prioritizing multiple criteria[17]. The Pareto frontier maps a surface in which all solutions are considered equivalent (non-dominant)—where an increase in one objective leads to a decrease in at least one or more other objectives. However, finding a Pareto optimal solution becomes difficult when many objectives are considered[56], hence a vector scalarization procedure is used[37]. Multi-objective prioritization is performed using vector scalarization, by describing the calculated parameters for a compound (A) as a multi-dimensional coordinate. The results are ranked by the magnitude of the vector $||a||$ between the multi-dimensional coordinates of predicted values of the chemical structure of a compound (A) and the defined ideal achievement objective point, (O), with the shortest vector length closest to the ideal in multi-dimensional space, being ranked the highest:

$$\|a\| = \sqrt{\sum_{p=1}^{n} (x_O{}^p - x_A{}^p)^2}$$

in which the ideal achievement objective point has the coordinates $(x_O^1, \ldots, x_O^n)$, and calculated values of the compound A form the coordinates $(x_A^1, \ldots, x_A^n)$.

For subsequent generations, prioritized individuals with calculated properties and parameters that satisfy defined thresholds are assigned to an elite population (P_E), and those that fail are assigned to a non-elite population (P_N), of which n random members form a random population (P_R). For all the calculations performed, P_E has a maximum size of 10,000 and P_R a maximum size of 500. The new parent population ($P_{P(G=n+1)}$) is created by merging P_E and P_R (that is, $P_{P(G=n+1)} = P_{E(G=n)} + P_{R(G=n)}$). This new population is subjected to another transformation process. The new parent population P_P from each generation is also added to a combined pool of all observed parents (P_{Pall}).

The population of transformed compounds from the last iteration and the pooled parent population are combined and all duplicates and compounds failing structure valency rules are removed to produce a merged population (P_M) of unique members ($P_M = P_{Pall} + P_T$). Properties and parameters (for example, Bayesian activity models values, physicochemical properties and predicted ADME properties) are calculated for each individual in P_M. Each member population P_M is evaluated against the achievement objectives $\{x_O^1, \ldots, x_O^n\}$, as described above. The entire process is repeated until a stop condition is satisfied.

Novelty is assessed by comparing the generated compound with compounds in ChEMBL, either as an exact match or by comparison of the Murcko framework[41], depending on whether the objectives are defined in terms of new compounds or new chemotypes. Novelty is filtered depending on the goals. ADME properties and CNS penetration are calculated using previously publishing Gaussian process models[57,58] as implemented in StarDrop (Optibrium). A synthetic accessibility score, representing historical synthetic knowledge, is calculated using a previously published algorithm[39]. The synthetic accessibility score combines the observation of fragments in ChEMBL and a complexity penalty. A limitation of the ECFP6-Bayesian prediction method is that fingerprints cannot distinguish stereochemistry if the stereochemistry is not encoded in the training data. In the ChEMBL database only 43% of the chiral compounds with chiral centres have their stereochemistry fully defined, thus it is not possible to distinguish between *R*

and *S* enantiomers. To reduce the complexity of synthesis, compounds with two or more chiral centres were filtered from the final population.

Receptor profiling. The detailed experimental protocols for the radioligand and functional receptor assays are available on the NIMH PDSP website (http://pdsp.med.unc.edu/UNC-CH%20Protocol%20Book.pdf).

hERG assay. Activity of the potassium channel hERG was assayed by the patch clamp method on a PatchXpress platform and by FluxOR Tl^+ assays. Assays were performed as previously described[47].

Metabolic stability assay. Metabolic stability was assessed, generating the *in vitro* intrinsic clearance (Cl_i) following incubation of test compound with mouse hepatic microsomes. The assay was performed as previously described[48].

Brain penetration measurement. Mice were housed under standard conditions: 12 h:12 h light–dark cycle and food and water available *ad libitum* throughout the study. The Drug Discovery Unit at the University of Dundee is dedicated to the humane care, maintenance and use of research animals and maintains compliance with UK Home Office regulations. All experiments were approved by the local ethical review committee. The ratio of test compound between brain and blood was assessed following intravenous administration to the female NMRI mouse.

Behavioural testing. Adult male and female C57BL/6J, D4R-KO mice (Jackson Laboratory), and PC7-KO mice were used. PC7 mice were backcrossed with C57BL/6J mice for more than ten generations. Animals were maintained in a humidity- and temperature-controlled room under a 14 h:10 h light–dark cycle (lights on at 8:00). All studies were conducted during the light cycle, between 10:00 and 16:00 in the following order: zero maze, open field and hole-board. All tests were separated by at least by 7 days. Animals were assigned to vehicle (0.1% DMA with 15% 2-hydroxypropyl-β-cyclodextrin (Sigma-Aldrich)) or compound **13**-treated groups, and were maintained in these groups throughout the experiments. Water and laboratory chow were supplied *ad libitum*. All experiments were conducted with an approved protocol from the Duke University Institutional Animal Care and Use Committee and according to the NIH Guide for the Care and Use of Laboratory Animals. To overcome the high intrinsic clearance in mouse hepatic microsomes of compound **13** ($Cl_i = 13.8\ ml\ min^{-1}\ g^{-1}$), mice were injected intraperitoneally with vehicle, or 0.7 or 1 $mg\ kg^{-1}$ of compound **13** and placed immediately into the open field for 60 min as described[49]. Activity was monitored as distance travelled and time spent in the centre zone. In the hole-board and zero-maze tests[49,50] mice were injected intraperitoneally with vehicle or compound **13** and tested 30 min later. Hole-board test responses were video taped for 10 min using high-resolution low-light cameras (Panasonic) and were scored using the TopScan program (Clever Sys) for the rate of head-pokes into the 16 holes. Zero maze behaviours were video taped over 5 min and were scored by trained observers blinded to the genotype, sex and treatment-condition of the animals using the Observer XT10 program (Noldus Information Technology) for the percentage of time in the open areas. All behavioural data presented as mean ± s.e.m. and were analysed by analysis of variance (ANOVA) and repeated measures ANOVA followed by Bonferroni corrected pair-wise comparisons (IBM SPSS 20). $P < 0.05$ was considered significant.

51. Glick, M., Jenkins, J. L., Nettles, J. H., Hitchings, H. & Davies, J. W. Enrichment of high-throughput screening data with increasing levels of noise using support vector machines, recursive partitioning, and laplacian-modified naive bayesian classifiers. *J. Chem. Inf. Model.* **46,** 193–200 (2006).
52. Rogers, D. & Hahn, M. Extended-connectivity fingerprints. *J. Chem. Inf. Model.* **50,** 742–754 (2010).
53. Truchon, J. F. & Bayly, C. I. Evaluating virtual screening methods: good and bad metrics for the "early recognition" problem. *J. Chem. Inf. Model.* **47,** 488–508 (2007).
54. Zhao, W., Hevener, K. E., White, S. W., Lee, R. E. & Boyett, J. M. A statistical framework to evaluate virtual screening. *BMC Bioinformatics* **10,** 225 (2009).
55. Cannon, E. O., Nigsch, F. & Mitchell, J. B. A novel hybrid ultrafast shape descriptor method for use in virtual screening. *Chem. Cent. J.* **2,** 3 (2008).
56. Corne, D. W. & Knowles, J. D. in *Proc. 9th Annual Conf. Genetic Evolutionary Computation* 773–780 (ACM, 2007).
57. Obrezanova, O., Csanyi, G., Gola, J. M. & Segall, M. D. Gaussian processes: a method for automatic QSAR modelling of ADME properties. *J. Chem. Inf. Model.* **47,** 1847–1857 (2007).
58. Obrezanova, O., Gola, J. M. R., Champness, E. J. & Segall, M. D. Automatic QSAR modeling of ADME properties: blood-brain barrier penetration and aqueous solubility. *J. Comput. Aided Mol. Des.* **22,** 431–440 (2008).